https://doi.org/10.46813/2023-146-096

TiO_2-2 RADIATING DAMAGES AS A RESULT OF THE IRRADIATION HELIUM IONS WITH ENERGIES OF 0.12 AND 4 MeV ON THE LINEAR ACCELERATOR

V.I. Butenko[1], A. Cenian[2], O.F. Dyachenko[1], O.V. Manuilenko[1], K.V. Pavlii[1], M. Sawczak[2], B.V. Zajtsev[1], V.I. Zhurba[1]
[1]National Science Center "Kharkov Institute of Physics and Technology", Kharkiv, Ukraine;
[2]Institute of Fluid-Flow Machinery, Polish Academy of Sciences, Gdansk
E-mail: dyachenkoa@kipt.kharkov.ua

On the linear accelerator of helium ions, the irradiation of TiO_2-2 samples with ions energy of 0.12 and 4 MeV to doses of $\approx 1 \cdot 10^{18}$ ion/cm^2 is executed. The elemental composition of TiO_2-2 samples is made by roentgen-fluorescence method. After irradiation a change of electrophysical characteristics is investigated, microscopic researches on electronic and optical microscopes are conducted. Numerical calculations of atom sputtering ratios taking into account of input angles of helium ions in a sample, and also phonons formation, atoms redistribution (segregation), appearance of the vacancies and displacements in TiO_2-2 sample are made. Processes of the flaking formation are investigated, and also presence of the metallization effect and long-range interaction effect in the irradiated samples is shown.

PACS: 29.17+w, 29.27 Bd

INTRODUCTION

In nuclear power plants ceramics is used as a thermal protection (Al_2O_3, SiO_2), nuclear fuel (UO_2, PuO_2), materials of the regulating units (B_4C, Sm_2O_3), slowing down and reflecting materials (BeO, ZrO_2, Be_2C), materials of the neutron protection (B_4C, HfO_3, Sm_2O_3), electroisolation in an active zone (Al_2O_3, MgO), fuel element covers (SiC, Si_3N_4).

In thermonuclear power ceramics plan to use for thermal and electric isolation of the first wall of the plasma chamber (SiC, Si_3N_4), plasma restrictions (SiC, Al_2O_3, B_4C), neutron protection (blankets from $LiAlO_2$, Li_2SiO_3, Li_2O), as a material for windows of the various frequency plasma heating (Al_2O_3, BeO) and etc.

Titan dioxide (TiO_2) is widely used in the chemical techniques, instrument making and medicine. Possessing properties of the semiconductor with *n*-conductivity, TiO_2 is a perspective material for formation of the solid electrolytes and materials which possess catalytic properties. Wide use TiO_2 as solid electrolyte is prevented its big resistance (10^{13} Ω/cm).

Analysis of TiO_2 properties and methods of its synthesis [1] point out the possibilities to change ionic conductivity by introduction in structure TiO_2 the oxides SnO, Co_2O_3, Sb_2O_5, AgO which have higher conductivity. The same effect as it will be resulted below, is reached by TiO_2 helium ions irradiation without addition of an exterior compounds. On a conductivity change it's possible to judge about physical-chemical processes proceeding in irradiated materials, in particular. The knowledge of conductivity change dependence from an irradiation dose and a current density of helium ions allow to create ionic current gauges, to control process of materials processing in extreme conditions and etc.

The odd researches spent on semiconductors [2, 3] or separate metals and alloys [2, 4 - 7] are devoted the description of an impacts of continuous and pulse electronic and ionic beams on a surface change of the irradiated materials. The numerous publications analysis has shown that at processing by ionic beams of solids for the purpose of their modification the ionic beams with energy from a hundred kiloelectronvolts to several megaelectronvolts are applied. Beams of easy ions (protons, helium, carbon, nitrogen, boron, oxygen, their mixture and combination) have appeared the most effective as, on the one hand, in comparison with heavy ions it's easier to receive, and, on the other hand, they have essentially big runs in a target. Ionic beams are capable to create in near-surface layers of materials the ultra-fast heating and superhigh-speed cooling ($\Delta T/\Delta t \sim 10^8 \ldots 10^{11}$ K/s). The temperatures gradient thus on a surface and in near-surface target layers can make 10^9 K/m. It leads to changes of a structure and properties of processed materials. At impact of ionic beams on a solids surface the defining factors influencing of a surface morphology and on a dynamics of structurally-phase transformations, occurring in a surface layers, are spatio-temporal distribution of an energy release power: density of the brought energy, action time, heating, melting, evaporation, ablation, thermal stress and shock wave.

The surface defines many properties of solids. So, for example, electric properties of semiconductors and dielectrics depend on composition and structure of a surface layer and define the wear resistance and corrosion resistance, an endurance limit, the heat resistance, etc. At processing of the dielectrics and semiconductors surface by ionic beams the morphological changes and modifications of its element composition take place.

In this work an irradiation parameters of TiO_2-2 samples on the linear accelerator of helium ions and methods of their measurement are described. Primary radiating characteristics and atom sputtering ratios are calculated. Experimental results of electrophysical properties TiO_2-2 are received and presence of metallization effect and long-range action effect in the irradiated samples is shown.

1. SOURCE AND PARAMETERS OF THE IRRADIATION, THE SAMPLE CHARACTERISTICS

In NSC KIPT the linear accelerator of helium ions (He^+) with energy of 0.12…4 MeV [8 - 10] works. Basic elements of the linear accelerator of helium ions are: injector, resonator with the accelerating structure, placed in a vacuum casing, and system of a beam formation and transport from output of the accelerating section to the irradiation chamber with accompanying diagnostic devices for carrying out of experimental works.

Feature of the interdigital accelerating structure of the section linear accelerator of helium ions is use of the alternating-phase focusing variant with step-by-step change of a synchronous phase and accruing amplitude of a RF field in accelerating gaps on a grouping area of the accelerating-focusing path. New effective inductance-capacitor adjusting devices ('contrivances') for this section in a form of rods located on a side of drift tubes, opposite to their suspension brackets are developed [10 - 13].

For an irradiation and studying of constructional material characteristics on the accelerator the special chamber and system of the experimental parameters measurement [14, 15] are created. Vacuum in the chamber is carried out with the help of the fore vacuum and turbo-molecular pumps, it provides without the oxygen environment in the chamber volume and the same vacuum as in accelerating structure. A temperature of irradiated samples is set by the heating element located directly in the irradiation chamber and measured by the thermocouple attached to the sample backside. The digital oscillograph ZET-302 and DAC/ADC ZET-210 for registration of irradiated sample parameters which are connected to the computer with the further data recording and their processing are used.

For change (increase/decrease) of the beam current density falling on a sample and shortening of an irradiation time, in front of the irradiation chamber the focusing triplet which allows changing beam radius, and, hence, a current density depending on requirements of an experiment is established [16]. A system of the beam formation and transport from accelerating section output to the irradiation chamber is shown in Fig. 1. Photos in absence of a current in triplet quadrupole lenses and at a currents selection are shown in Figs. 2, 3. The chosen focusing system has allowed increasing density of a beam helium ions current in several times (to 7).

Currents of ions beam are measured by means of the induction contactless flying gauges established on an input and output from a triplet, and also directly ahead of the irradiated sample [17].

Table 1

Irradiation parameters

Parameter	Value
Beam energy, MeV	0.12…4
Pulse current, μA	1100…300
Pulse length, μs	500
Repetition rate, imp./s	2…5
Sample temperature, °C	up to 900

Basic parameters of helium ions beam at an irradiation of samples on the linear accelerator are resulted in Table 1. Diameter of helium ions beam made ~15 mm, it corresponds to TiO_2-2 irradiated samples.

TiO_2-2 samples (diameter is 19.6 mm, thickness is 1.00 mm and weight is 1.0459 g) have been chosen for an irradiation. The samples elemental composition was defined by X-ray fluorescent method which is based on dependence of X-ray fluorescence intensity on the element concentration in a sample. Impurities composition in TiO_2-2 sample (a basic element – 95.096%) in percent is following: Si-2.325, S-0.222, Cl-0.262, Ca-0.067, V-0.895, Fe-0.936, Ni-0.016, Cu-0.055, Zr-0.007, Nb-0.010, Mo-0.009, Pb-0.013, Sn-0.023, I-0.065. TiO_2-2 sample surface and its appearance are shown in Fig. 4.

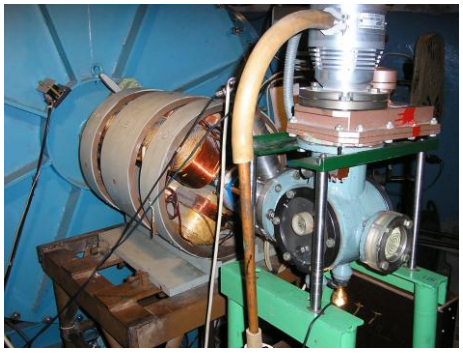

Fig. 1. System of the beam formation and transport from accelerating section output to the irradiation chamber

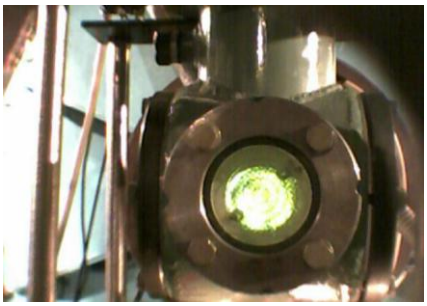

Fig. 2. Accelerated beam visualization in absence of a current in triplet quadrupole lenses

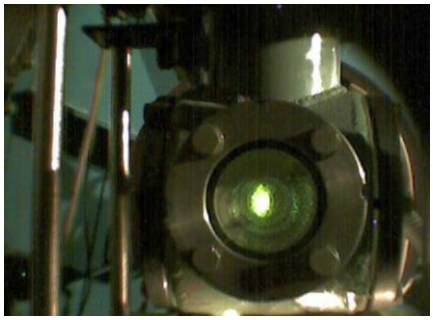

Fig. 3. Accelerated beam visualization at currents selection in quadrupole lenses (spot diameter of ~1 cm)

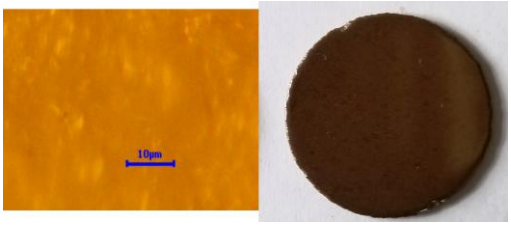

Fig. 4. TiO_2-2 sample surface and appearance

The conducted microscopic research of samples surface has not shown their roughness in limits of ± 0.1 Å.

2. IONIZATION, SEGREGATION, FORMATION PHONONS, VACANCIES AND DAMAGEABILITY

For calculation of the ions range in solids the SRIM software package [18, 19] was used which allows to receive following information about: vacancies distribution in a target; redistribution of irradiated material atoms (segregation); sputtering ratios; phenomena connected with ions energy loss; distribution of ionization and phonons formation. These are 'primary' characteristics which define processes dissociation, radiating diffusion of the sample elements, distribution of elastic waves and etc.

Calculations in the SRIM program taking into account of the displacement cascades were spent. Energy losses going on the ionization, phonons formation and damageability by a beam of helium ions and the displacement cascades for irradiation energies of 0.12 and 4 MeV are resulted in Table 2.

Table 2

Calculated characteristics of the samples

Energy, MeV	Energy loss, %		
	Ionization	Phonons	Damageability
	He^+/cascade	He^+/cascade	He^+/cascade
TiO_2			
0.12	93.7/1.10	0.78/4.15	0.08/0.20
4	99.68/0.07	0.04/0.20	0.00/0.01
TiO_2-2			
0.12	93.85/1.00	0.77/4.12	0.08/0.18
4	99.69/0.06	0.04/0.20	0.00/0.01

Energy absolute values for TiO_2 and TiO_2-2, going on these processes are resulted in Table 3. Energy values for pure TiO_2 and TiO_2-2 are almost identical. It means that in certain cases it's possible to use calculations nonmetering of additives in TiO_2-2.

Table 3

Energy values going on the ionization, phonons formation and damageability

Energy, MeV	Energy, keV/ion		
	Ionization	Phonons	Damageability
TiO_2			
0.12	113.7	5.9	0.34
4	3990.0	9.6	0.51
TiO_2-2			
0.12	113.8	5.9	0.31
4	3990.0	9.5	0.50

As appears from Tables 2, 3 a most part of a beam energy goes on the ionization. The basic contribution to phonons formation and damageability occurs at the expense of displacement cascades. On phonons formation at beam energies of 0.12 and 4 MeV it's spent at 17-19 times more energy, than for damageability. Hence, the role of phonons and ionization in some radiating effects can be defined. The profiles of ionization, phonons formation, segregation and helium occurrence, vacancies formation in TiO_2-2 at energies 0.12 and 4 MeV, accordingly, are resulted in Figs. 5, 6, in relative units.

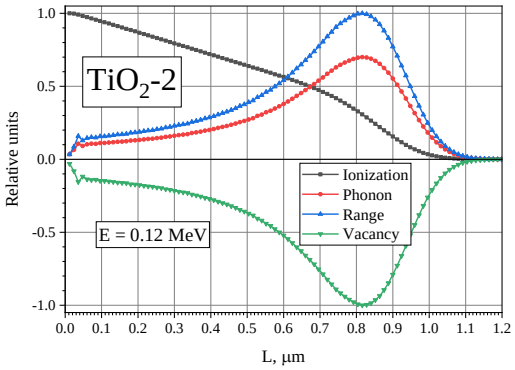

Fig. 5. Profiles of the ionization, segregation, phonons formation and vacancies in TiO_2-2, E = 0.12 MeV

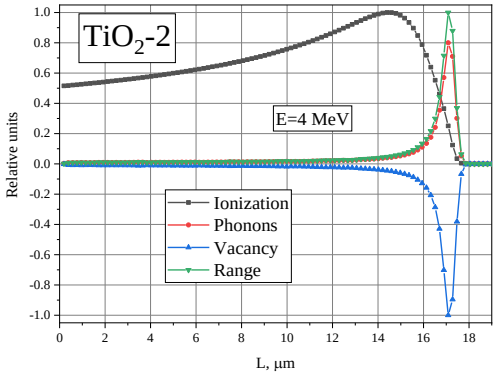

Fig. 6. Profiles of the ionization, segregation, phonons formation and vacancies in TiO_2-2, E = 4 MeV

As segregation atoms play a dominant role in change of the thermalphysic and electrophysical characteristics of ceramic materials, relations of TiO_2-2 redistributed atoms to helium atoms are presented in Table 4.

Table 4

Relations of TiO_2-2 redistributed atoms to helium atoms

E = 0.12 MeV				
O/He	Ti/He	Si/He	S/He	Cl/He
64.44	42.85	1.68	0.096	0.113
Ca/He	V/He	Fe/He	Cu/He	
0.030	0.380	0.408	0.023	
E = 4 MeV				
O/He	Ti/He	Si/He	S/He	Cl/He
99.90	69.13	2.67	0.152	0.181
Ca/He	V/He	Fe/He	Cu/He	
0.048	0.614	0.661	0.039	

Other elements bring the insignificant contribution to the segregation process.

Vacancies formation and quantity of displacement on an ion in TiO_2-2 samples play a dominant role in damageability calculations (dpa – quantity of displacements per atom). This data has been received at processing of calculations in the SRIM program.

For damageability calculation (dpa) and damageability distribution profile the curves of Figs. 5, 6 *Vacancies* and an expression, given lower, were used:

$$dpa = \frac{D_{ion} \cdot dpi}{N_m} = \frac{D_{ion} \cdot dpi}{N_A \cdot m_{mole}},$$

where D_{ion} is a radiation dose [ion/cm^2] (an experimental parameter), dpi is a quantity of displacements per ion (from SRIM calculations), N_A is the Avogadro number, $m_{mole} = \frac{m}{M}$, $m = \rho_0 \cdot SL$, where ρ_0 is the sample measured density, S = 1 cm^2 is the sample unit area, L is the maximum ions range in a sample, $M = \frac{1}{100}\sum_i \mu_i n_i$ is the sample molar mass, μ_i is the molecular weight of *i-th* element sample, n_i is percentage *i-th* element of a sample. Final expression for calculation of displacements per atom (dpa) looks like:

$$dpa = \frac{D_{ion} \cdot dpi}{N_A \cdot \rho_0 \cdot SL} \cdot \frac{1}{100}\sum_i \mu_i n_i .$$

Damageability (dpa) for E = 0.12 MeV has made ≈ 49 displacements/atom, for E = 4 MeV has made ≈ 5.0 displacements/atom (for irradiation doses of 10^{18} ion/cm^2). The calculated damageability (dpa) profiles for TiO_2-2 samples at helium ions energies of 0.12 and 4 MeV are resulted in Figs. 7, 8.

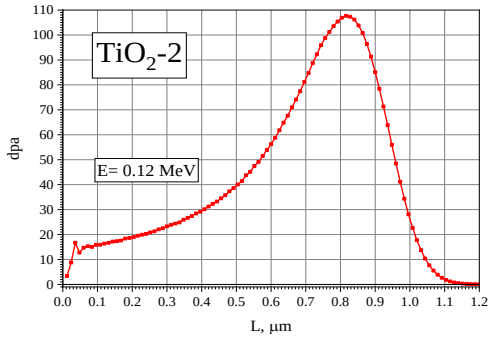

Fig. 7. Profile of the displacements formation in TiO_2-2 sample at helium ions irradiation with E = 0.12 MeV

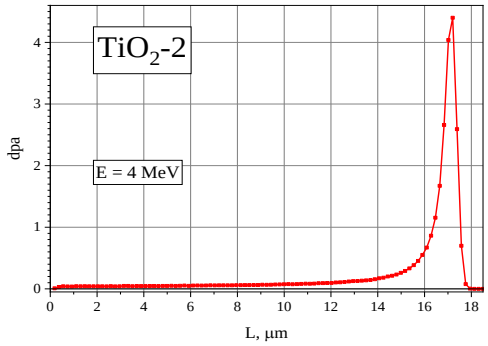

Fig. 8. Profile of the displacements formation in TiO_2-2 sample at helium ions irradiation with E = 4 MeV

As follows from the spent calculations the phonons formation occurs in areas of ionization, segregation and vacancies formation; ionization occurs basically before phonons formation, segregation and vacancies formation. Since samples at irradiation are earthed and electrons mobility more than in 5000 times more ions mobility the ionization area will be positively charged.

Hence, the accelerated ions irradiation leads to formation of a considerable quantity of radiating defects in a thin surface layer of a substance and causes change of the chemical composition of this layer as at the expense of ions penetration (an ion-implantation doping), and at the expense of change of the chemical elements concentration which are a part of targets (if they consist of two or more components). Formation of radiating defects and chemical composition change stimulate passing of secondary processes [7], such as formation of new crystal phases, amorphous layers, micro voids and etc.

From the spent calculations follows that energy expended for the ionization in samples volume is equal ≈ 94% for 0.12 MeV and 99.7% for 4 MeV and occurs mainly at the expense of helium ions. Formation of vacancies and phonons take place mainly at the expense of displacement cascades. As a segregation occurs mainly after ionization process and electrons mobility is a minimum in $5 \cdot 10^3$ times above ions mobility, there is a polarization of the redistributed atoms in a sample volume with their following acceleration. This process changes electrophysical, thermalphysic and other characteristics of irradiated samples. Phonons formation at samples irradiation create an additional excitation collective mode, it results as in change of some characteristics of irradiated samples. All these effects as it will be shown below, lead to blistering and flaking formation both on an irradiated surface, and on the back (not irradiated) side of samples.

3. SPUTTERING RATIOS

For calculations of sputtering ratios also the SRIM program has been used which with adequate accuracy considering the displacement cascades, counts sputtering ratios of the all atoms of TiO_2-2 ceramics structure. Since for sputtering the cascades which come back to a target surface are important for a sputtering calculation the small surface layer of a sample is enough to use. The necessary thickness of samples for calculations was estimated at start some fast examples and, having looked on what depth efficiency of a sputtering remains to a constant, this value selected. For cascades in a target at very low energy which is a sputtering major factor, the SRIM a hard-sphere model for scattering uses. For definition of an optimum quantity of helium ions at calculation of atoms sputtering of TiO_2-2 samples the calculations in the SRIM program are made at doses to $9 \cdot 10^6$ particles. The sufficient number of helium ions for calculations in the SRIM program makes ≈ $(3…5) \cdot 10^6$ for energies 0.12 and 4 MeV. The scheme of calculations in the SRIM program is presented in Fig. 9 (with indication of an entry angle of helium ions beam in a sample).

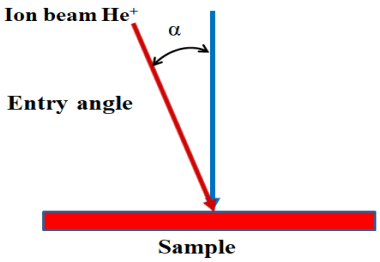

Fig. 9. Scheme for calculations in the SRIM program

In the beginning calculations for TiO_2-2 have been carried out at α = 0°. Change of a total sputtering ratio on a sample depth for energy of helium ions beam of

4 MeV is shown in Fig. 10. The same calculations have been made for E = 0.12 MeV.

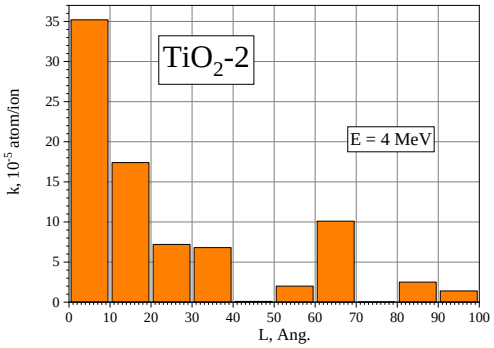

Fig. 10. Change of a total sputtering ratio on TiO_2-2 sample depth for energy of helium ions beam of 4 MeV

Change of sputtering ratios O and Ti, basic elements, is resulted in Fig. 11. The contribution to a total sputtering ratio of TiO_2-2 other elements is less 1%.

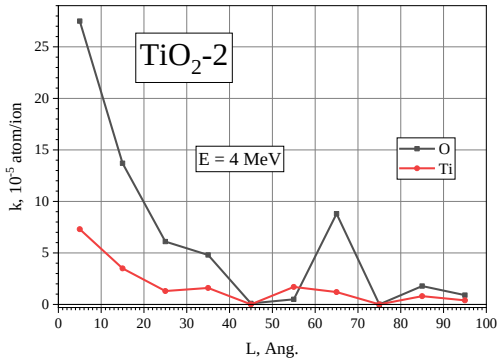

Fig. 11. Change of sputtering ratios O and Ti on TiO_2-2 sample depth for energy of helium ions beam of 4 MeV

Sputtering occurs when the cascade of displacement atoms gives to a target atom the energy exceeding the surface binding energy (≈ 3.5 eV). That there would be a sputtering, the atom energy directed perpendicularly to a sample surface should be above surface energy. Hence, for sputtering only displacement cascades which come back to a target surface are important.

For helium ions energy of 0.12 and 4 MeV, at α = 0°, total sputtering ratios are following:

$k \approx 83 \cdot 10^{-5}$ atom/ion, E = 0.12 MeV;

$k \approx 0.1 \cdot 10^{-5}$ atom/ion, E = 4 MeV.

However, in process of a dose set a sample the target becomes rough, efficiency of a sputtering will increase, as each surface atom is connected with a surface smaller electron quantity. Calculation of a sputtering at α = 0° does not include effects of a roughness change which changes in time irradiation. At change of a surface binding energy, a sputtering efficiency will increase no more than in 2 times regardless of a fact that occurs with irradiated surface.

At TiO_2-2 irradiation on the linear accelerator of helium ions with energies of 0.12 and 4 MeV a surface change occurs, at the expense of a blistering and flaking formation, and as a result of structure atoms of samples sputtering also. So, after TiO_2-2 irradiation the surface micrographs have been made. A surface structure of TiO_2-2 irradiated sample is resulted in Fig. 12.

After irradiated sample micrographs processing the dependence of a roughness along of TiO_2-2 surface has been received (Fig. 13).

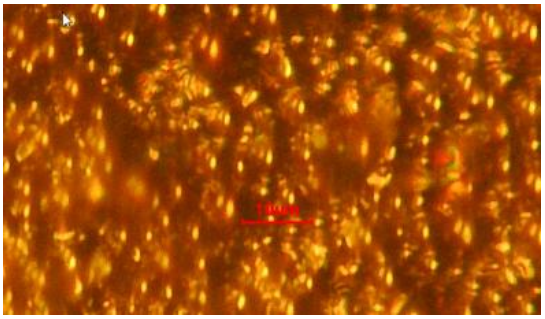

Fig. 12. TiO_2-2 surface structure. E = 0.12 MeV, an irradiation dose was ≈ $1.2 \cdot 10^{18}$ ion/cm^2

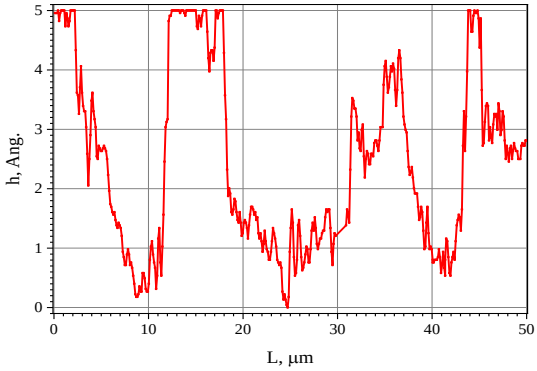

Fig. 13. Dependence of a roughness of TiO_2-2 irradiated sample on a length of its surface. E = 0.12 MeV, an irradiation dose was ≈ $1.2 \cdot 10^{18}$ ion/cm^2

From the resulted data (see Figs. 12, 13) it's visible that a surface is non-uniform, have a developed relief, the hollows maximum depth is no more than 5 Å. And with relief change of samples surface at an irradiation the entry angle of helium ions changes and the sputtering ratio of TiO_2-2 elements can change. At calculations in the SRIM program these facts have been considered by means of ions entry angle change in irradiated samples and the hollows maximum depth.

In Table 5 values of TiO_2-2 sputtering ratios are resulted at entry angles of helium ions beam of 0…90° and the maximum value of the hollows depth of 5 Å.

Table 5

TiO_2-2 total sputtering ratios at E = 0.12 MeV and E = 4 MeV

$k \cdot 10^{-2}$ atom/ion, E = 0.12 MeV								
α°	0	6	12	18	24	30	36	42
k	1.9	1.92	1.93	2.25	2.26	2.24	2.23	2.20
α°	48	54	60	66	72	78	84	89
k	2.18	2.42	2.39	2.63	3.15	3.88	6.01	29.2
$k \cdot 10^{-5}$ atom/ion, E = 4 MeV								
α°	0	6	12	18	24	30	36	42
k	82.7	82.9	82.0	98.2	99.7	98.2	97.2	95.1
α°	48	54	60	66	72	78	84	89
k	92.7	103	102	111	137	165	255	1183

The dependences of the total sputtering ratios change on an entry angle of helium ions beams taking into account the hollows maximum depth of 5 Å and ion range of 100 Å are resulted in Figs. 14, 15.

The range of sputtering ratios changes at α = 0…90° has made:

E = 0.12 MeV, k = (1.9…29.2)·10^{-2} atom/ion;

E = 4 MeV, k = (83…1183)·10^{-5} atom/ion.

Average values of total sputtering ratios, disregarding extreme values, that is at α = 0° and α = 90°, are following:

E = 0.12 MeV, k = 2.6·10^{-2} atom/ion;

E = 4 MeV, k = 114·10^{-5} atom/ion.

Since at calculations the maximum hollows depth was used the averaging sputtering ratios on hollows depth is received:

E = 0.12 MeV, k = 1.3·10^{-2} atom/ion;

E = 4 MeV, k = 57·10^{-5} atom/ion.

We consider that it's the greatest possible sputtering ratios at E = 0.12 and E = 4 MeV.

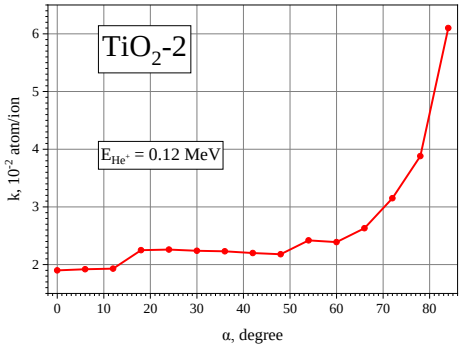

Fig. 14. Dependence of a total sputtering ratio on an entry angle of helium ions with E=0.12 MeV in TiO_2-2 sample

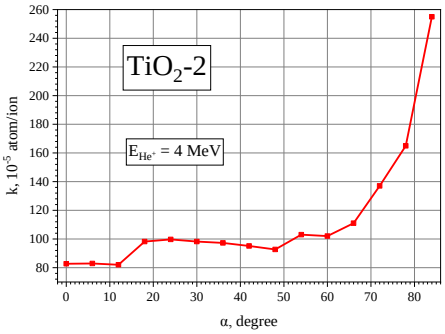

Fig. 15. Dependence of a total sputtering ratio on an entry angle of helium ions with E = 4 MeV in TiO_2-2 sample

4. EFFECTS OF TiO_2-2 METALLIZATION AND LONG-RANGE INTERACTION, ELECTROPHYSICAL CHARACTERISTICS AND SWELLING

We develop such experimental techniques of researches: microscopic, measurements of electrophysical characteristics and frictional parameters of ceramic materials, ultrasonic researches.

The technique of ceramic materials researches is following. After set a sample of an irradiation certain dose the microscopic researches are conducted which allow to study the blistering and flaking formations and their change dynamics from an irradiation dose and temperature, dimensional stability (swelling, sintering), grains size changes, to investigate a surface roughness and to study influence of dusting processes of various materials at an irradiation on the blistering and flaking dynamics.

For finding-out of a metallization effect formation in irradiated samples TiO_2-2 irradiation on the linear accelerator of helium ions with energy of 0.12 MeV has been made. The irradiation dose has made ~1.2·10^{18} ion/cm^2, a temperature was ≈ 60°C. The observed effect of a surface metallization of TiO_2-2 sample irradiated surface is shown in Fig. 16.

The surface linear profile in the metallization area of TiO_2-2 irradiated sample in a red spectrum is shown in Fig. 17.

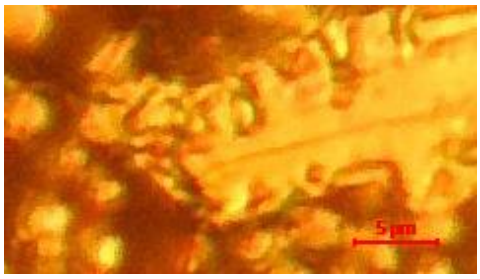

Fig. 16. Metallization surface of the irradiated sample

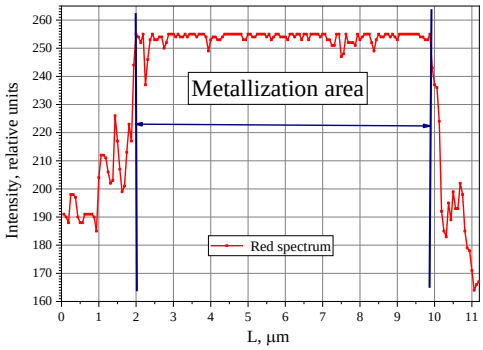

Fig. 17. Spectrum of TiO_2-2 surface in the metallization field after irradiation by helium ions with E = 0.12 MeV

It's possible to explain metallization effect TiO_2 dissociation with the subsequent of titan and oxygen diffusion to a sample surface. At an irradiation of TiO_2-2 sample by helium ions with energy of 4 MeV a surface metallization was not revealed. As the segregation of TiO_2-2 elements at energy of 4 MeV is maximum on depth of 14…18 μm (see Fig. 6), and at E = 0.12 MeV a segregation maximum is located on a depth 0.1…1.1 μm (see Fig. 5) for revealing of a surface metallization, it's necessary to increase an irradiation dose and an irradiation to spend at more high temperature. Under existing conditions of an irradiation (E = 4 MeV), it's necessary to expect that owing to TiO_2 dissociation in an irradiated sample volume the electrophysical characteristics will change.

After samples irradiation by helium ions a certain dose with energy of 4 MeV the surface electroresistances of a front side and a back side of samples, the volume electroresistance were measured, the microscopic researches on optical and electronic microscopes were conducted. After measurements there was a further irradiation of these samples with subsequent measurements. Surfaces of the front side (irradiated) and the back side (not irradiated) of TiO_2-2 sample are resulted in Figs. 18, 19. A dose of an irradiation was ~1.2·10^{18} ion/cm^2, a temperature was ≈ 60°C.

From the photos made on optical and electronic microscopes, it's visible that the surface is non-uniform, has the developed relief on which concentric traces from an ionic beam and craters, splashes of a sample material and metallization area with small grains are looked.

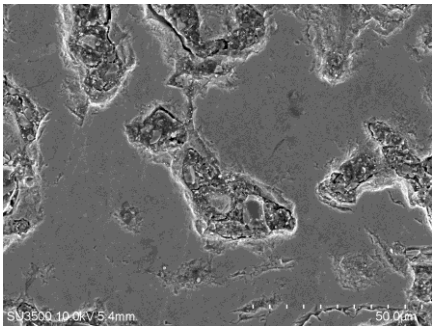

Fig. 18. Front side of TiO_2-2 irradiated sample (E = 4 MeV)

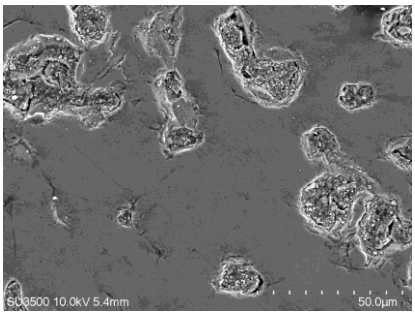

Fig. 19. Back side of TiO_2-2 irradiated sample (E = 4 MeV)

The flaking formation both on the front side and on the back side of a sample is clearly visible. The blistering formation on the front side and the back side of the irradiated samples is not observed. The flaking filling ratios $k=S/S_0$, where S is a surface area of a sample, flaking occupied; S_0 is the irradiated front side or back side of a sample have been calculated. Dependences of the flaking filling ratios from an irradiation dose are shown in Fig. 20.

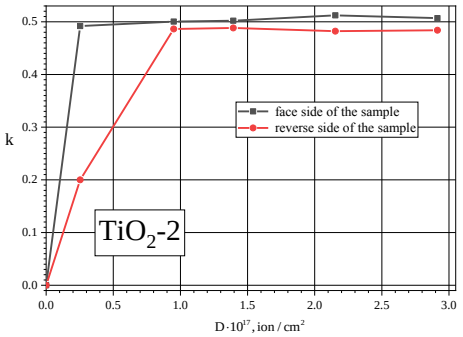

Fig. 20. Dependences of the flaking filling ratios from an irradiation dose of the front side and the back side of TiO_2-2 sample

From Fig. 20 follows that at an irradiation dose of ~$1 \cdot 10^{17}$ ion/cm^2, the surface areas values of a flaking formation practically coincide. However, the flaking depth on the front side of a sample is approximately twice more than on the back side. More careful research, further, will be given this point in a question.

After each irradiation gathered dose the surface and volume electroresistances have been measured. These dependences on an irradiation dose are resulted in Figs. 21, 22, accordingly. Initial values of the surface and volume electroresistances of not irradiated samples are indicated on figures.

From the mentioned results follows that electroresistance change, both on the front side and on the back side of TiO_2-2 sample, occurs owing to basic elements dissociation. It's necessary to notice that after each irradiation session the exposure of samples was made. Then the surface and volume electroresistances were measured. Partial restoration of the electroresistance no more than 5% has been registered.

From the mentioned results on measurements of the flaking change and electroresistance follows that there is an effect of the long-range interaction. To experimental and theoretical researches of this effect are devoted numerous works [20 - 24]. However, for today there is no unambiguous mechanism explaining this effect. In our opinion, it's possible to explain effect of the long-range interaction by complex action on a sample surface, namely, generation of thermoelastic tensions and shock waves, at the expense of the formation and distribution phonons and stimulating diffusion of impurities, as on interstices, and to borders of grains.

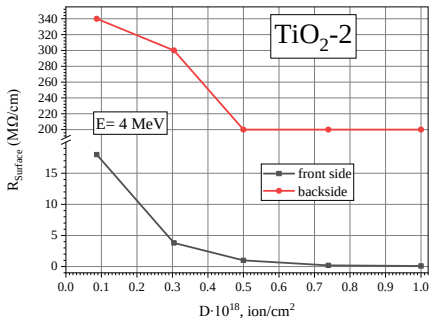

Fig. 21. Dependences of TiO_2-2 surface electroresistance on an irradiation dose. Initial value was 20 GΩ/cm (on the front and back sides of a sample)

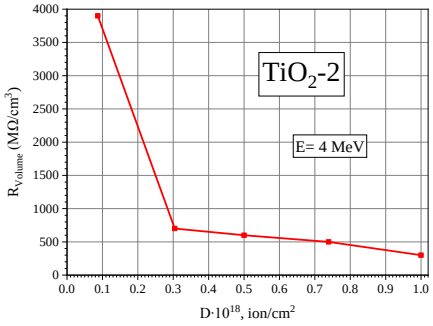

Fig. 22. Dependence of TiO_2-2 volume electroresistance on an irradiation dose. Initial value was 50 GΩ/cm^3

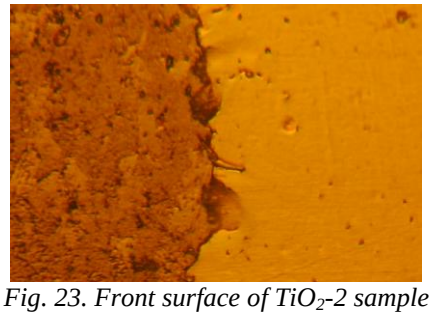

Fig. 23. Front surface of TiO_2-2 sample

As at TiO_2-2 irradiation at a dose of ~$1 \cdot 10^{18}$ ion/cm^2 a swelling of a sample material was revealed. The photo of a sample front surface is resulted in Fig. 23. The sample right part is not irradiated surface; left part is the irradiated surface.

Analysis has shown that a swelling value is order of 1 μm, at an irradiation dose of ~$1 \cdot 10^{18}$ ion/cm^2. A swelling is connected with diffusion of gaseous elements (He, O) to a surface at the expense of internal bubbles formation and grains growth.

CONCLUSIONS

On the linear accelerator the irradiation of TiO_2-2 samples by helium ions with energies of 0.12 and 4 MeV is spent. For these energies the ionization profiles, formation of vacancies and phonons, redistribution of sample atoms and damageability are calculated. Also sputtering ratios taking into account change of a surface samples profile are calculated.

At E = 0.12 MeV more than 94% of energy goes on the ionization, an order of 5% on the phonons formation and less than 0.3% on a damageability. For E = 4 MeV, more than 99.7% of energy goes on the ionization, an order of 0.2% on the phonons formation and less than 0.02% on a damageability. Therefore, damageability for E = 0.12 MeV makes 49 displacements/atom, for E = 4 MeV is 5.0 displacements/atom.

Taking into account the displacement cascades the sputtering ratios of all atoms of TiO_2-2 ceramics structure have been calculated. Nonmetering of samples profile change, for energy of helium ions of 0.12 and 4 MeV, at an entry angle in samples $\alpha = 0°$, the total sputtering ratios are following: $k \approx 83 \cdot 10^{-5}$ atom/ion, E = 0.12 MeV; $k \approx 0.1 \cdot 10^{-5}$ atom/ion, E = 4 MeV. Taking into account change of samples profile for the entry angles of 0…90° the average sputtering ratios have made: E = 0.12 MeV, $k = 1.3 \cdot 10^{-2}$ atom/ion; E = 4 MeV, $k = 57 \cdot 10^{-5}$ atom/ion.

After TiO_2-2 irradiation the microscopic researches of the front side (irradiated) and the back side (not irradiated) of a sample have been conducted. The metallization effect on the front side of a sample (E = 0.12 MeV) which is possible to explain for the account TiO_2 dissociation with the subsequent diffusion of the titan to a sample surface is revealed. At E = 4 MeV the metallization effect was not found. This results from the fact that the segregation of TiO_2-2 elements at energy of 4 MeV is located on a depth of 14…18 μm, and at E = 0.12 MeV the segregation profile is located on a depth of 0.1…1.1 μm. For revealing of surface metallization it's necessary to increase an irradiation dose and an irradiation to spend at more high temperature.

Also at TiO_2-2 irradiation at an irradiation dose of ~$1 \cdot 10^{18}$ ion/cm^2 swelling of a sample material was revealed which is connected with diffusion of gaseous elements (He, O) to a surface at the expense of internal bubbles formation and grains growth.

An effect of the long-range interaction is defined by change (reduction) of the surface electroresistance both on the front side of a sample, and on the back side. Also the volume electroresistance decreases at increase of an irradiation dose. Besides, on both sides the flaking formation is observed. And, the flaking areas on the front side and back side of a sample increase with increase of an irradiation dose. It's possible to explain reduction of the surface and volume electroresistances TiO_2 dissociation. That is in all volume of an irradiated sample there is a metal (Ti), only it leads to electroresistance reduction. But there is a question, whence takes energy on the back side of a sample for the formation flaking and TiO_2 dissociation? TiO_2 binding energy an order of 12…15 eV, a thickness of a sample is ≈ 1 mm, and the helium ions range and primary processes formation area are no more than 18.5 μm. In our opinion, it's possible to explain a complex influence. First, the phonon excited propagation with additional frequency mode formation from helium ions beam. This energy has enough for TiO_2 dissociation and tensions formation on the back side of a sample. Secondly, in a sample ionization area the positive charge accumulates, under Coulomb field action there is a polarization of the segregation atoms and structure molecules. This energy has enough for acceleration of segregation atoms and structure molecules with formation of the cyclic primary processes. The essential role at the flaking formation is played by oxygen and helium diffusion. With increase of an irradiation dose appear diffused channels for oxygen and helium directly in the areas of the flaking formation (Fig. 24).

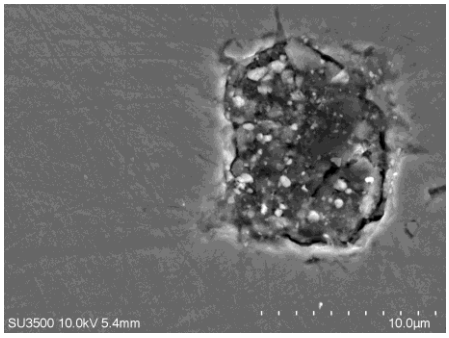

Fig. 24. Flaking formation with diffused channels

REFERENCES

1. H. Ullmaier. The influence of helium on the bulk properties of fusion reactor structural materials // *Nuclear fusion*. 1984, v. 24, № 8, p. 1039-1083.
2. J. Wesson. *Tokamaks*: 3rd ed. Oxford: Clarendon Press, 2004, 749 p.
3. *ITER physics basis, Nuclear Fusion*. 1999, v. 39, № 12.
4. V. Shakhnov, L. Zinchenko, I. Kosolapov, I. Filippov. Modeling and optimization of radiation tolerant microsystems // *Proc. EMS'14*. 2014, p. 484-489.
5. V.A. Belous, G.I. Nosov, N.A. Azarenkov. About influence of an irradiation by ions Ar+ on corrosion resistance of metals and alloys // *Surface Physical Engineering*. 2010, v. 8, № 2, p. 161-168.
6. K.V. Kosterin. Sputtering of solids by ionic bombardment: adatomic mechanisms and a possible role phonons // *Physics and Chemistry of Materials Processing*. 1995, № 3, p. 43-48.
7. L.B. Begrambekov. *Updating of solids surface at ionic and plasma influence*. M.:"MERI", 2001, 34 p.

8. V.O. Bomko, O.F. Dyachenko, O.M. Yegorov, et al. Development of investigations on the MILAC heavy ion linear accelerator // *Proc. of the LINAC08, Vancouver, Victoria, Canada*. 2008, p. 187-189.
9. S.N. Dubniuk, R.A. Anokhin, A.F. Dyachenko, et al. Radiation complex on the basis of helium ions linac // *Problems of Atomic Science and Technology*. *Series "Plasma Electronics and New Methods of Acceleration"*. 2018, № 4, p. 46-51.
10. A.F. Dyachenko. Interdigital structures of heavy ions linear accelerators: their tuning, beams focusing and use (review) // *Problems of Atomic Science and Technology. Series "Nuclear Physics Investigations"*. 2019, № 6, p. 17-22.
11. V.O. Bomko, O.F. Dyachenko, Ye.V. Ivakhno, et al. New prestripping section of the MILAC linear accelerator designed for accelerating a high current beam of light ions // *Proc. of the EPAC 2006 Edinburgh, Scotland.* 2006, p. 1627-1629.
12. V.O. Bomko, A.F. Dyachenko, B.V. Zajtsev, et al. Inductance-capacitor system for tuning of interdigital structure of the ion linear accelerator // *Problems of Atomic Science and Technology. Series "Nuclear Physics Investigations"*. 2007, № 5, p. 180-183.
13. V.O. Bomko, O.F. Dyachenko, Ye.V. Ivakhno, et al. Adjustment of a new pre-stripping section the multicharge ion linear accelerator (MILAC) // *Proc. of the 11-th European Particle Accelerator Conference EPAC08, Genoa, Italy*. 2008, p. 3410.
14. R.A. Anokhin, B.V. Zaitsev, K.V. Pavlii, et al. Experimental complex for investigation of construction materials on the helium ions linear accelerator // *Problems of Atomic Science and Technology*. *Series "Nuclear Physics Investigations"*. 2017, № 6, p. 167-171.
15. R.A. Anokhin, S.N. Dubniuk, A.F. Dyachenko, et al. Beam and target parameters measurement system on helium ions linear accelerator // *Problems of Atomic Science and Technology*. *Series "Plasma Electronics and New Methods of Acceleration"*. 2018, № 4, p. 30-35.
16. A.F. Dyachenko, R.A. Anokhin, S.N. Dubniuk, et al. The bunch formation and transport system to the target of the helium ions linac // *Problems of Atomic Science and Technology. Series "Plasma Electronics and New Methods of Acceleration"*. 2018, № 4, p. 52-55.
17. A.F. Dyachenko. The high-sensitivity induction gauge of a beam current of heavy ions linear accelerator // *The Journal of Kharkiv National University. Physical Series "Nuclei, Particles, Fields".* 2010, v. 1(45), № 887, p. 118-121.
18. http://www.srim.org.
19. B. Widrow, J.R. Glover, J.M. McCool, et al. Adaptive noise cancelling: principles and applications // *Proc. IEEE*, 63, p. 1692-1716.
20. Yu.P. Sharkeev, E.V. Kozlov, A.N. Didenko, et al. The mechanisms of the long-range effect in metals and alloys by ion implantation // *Surface and Coating Technology*. 1996, v. 83, p. 15-21.
21. Yu.V. Martynenko. Effects of long-range interaction at ionic implantation // *Results of science and technics*. M., 1993, v. 7, p. 82-112.
22. P.V. Pavlov, E.C. Demidov, V.V. Karzanov. Effect of long-range interaction in the silicon crystals alloyed by iron, depending on a dose and intensity of an irradiation argon ions // *Proc. of 9th All-Union conference "Interaction of nuclear particles with solid"*. M.: "MERI", 1989, v. 2, p. 84.
23. D.I. Tetelbaum, V.Ya. Bayankin. Effect of long-range interaction // *Nature*. 2005, № 4, p. 9-17.
24. V.Ya. Bayankin, M.I. Guseva, D.I. Tetelbaum, F.Z. Gilmutdinov. Segregation as demonstration of long-range interaction effect at an irradiation boron ions of the foils of permalloy-79 and Cu-Ni alloys // *Surface. X-ray, synchrotron and neutron researches*. 2005, № 5, p. 77-81.

Article received 28.05.2023

РАДІАЦІЙНІ ПОШКОДЖЕННЯ TiO_2-2 У РЕЗУЛЬТАТІ ОПРОМІНЕННЯ НА ЛІНІЙНОМУ ПРИСКОРЮВАЧІ ІОНАМИ ГЕЛІЮ З ЕНЕРГІЯМИ 0.12 І 4 МеВ

В.І. Бутенко, A. Cenian, О.Ф. Дьяченко, О.В. Мануйленко, К.В. Павлій, M. Sawczak, Б.В. Зайцев, В.І. Журба

На лінійному прискорювачі іонів гелію виконано опромінення зразків TiO_2-2 з енергією іонів 0,12 і 4 МеВ до доз $\approx 1 \cdot 10^{18}$ іон/см^2. Елементний склад зразків TiO_2-2 отримано рентгенофлюоресцентним методом. Після опромінення проведено мікроскопічні дослідження на електронному та оптичному мікроскопах, досліджено змінення електрофізичних характеристик. Зроблено числові розрахунки коефіцієнтів розпилення атомів з урахуванням кутів входу іонів гелію в зразок, а також утворення фононів, перерозподілу атомів (сегрегація), утворення вакансій і зміщень у зразка TiO_2-2. Досліджено процеси утворення флекінгу та показано наявність ефектів металізації й далекодії в опромінених зразках.